Charge Carrier Transfer across the Silica Nanoparticle/Water Interface

Timothy Schatz,[†] Andrew R. Cook,*[,‡] and Dan Meisel*[,†]

Chemistry Division, Argonne National Laboratory, Argonne, Illinois 60439

Received: May 5, 1998; In Final Form: July 6, 1998

We determined the yield of hydrated electrons, e^-_{aq}, in irradiated silica suspensions at very high particle concentrations. The initial concentration of e^-_{aq}, measured immediately after a pulse of high-energy electrons, increases with the silica loading, proportionately with the dose absorbed by the sample. Therefore, the yield of e^-_{aq} per unit energy absorbed remains unaltered even at 50% weight of silica. This observation holds for particles in the range of 7−22 nm in diameter. Under heavy loading of silica, a significant percentage of the energy is absorbed by the silica (essentially equal to the silica weight percent). Thus, our observations imply that energy that is originally deposited in silica crosses the solid−liquid interface and appears in the aqueous phase as solvated electrons. Possible mechanisms for this crossover process are discussed. It is proposed that either every electron that is generated in silica escapes to the water or that highly energetic secondary electrons are ejected from the silica particles and subsequently create spurs similar to those formed by primary electrons that initially are deposited in water.

Introduction

Absorption of ionizing radiation in condensed phases produces ionization and excitation events.[1] The specific effects depend on the nature of the radiation and the material. Owing to the technological importance of silica-based materials, the creation of charge carriers upon absorption of ionizing radiation in SiO_2 is well-established.[2−4] The majority of electron−hole pairs created by ionizing radiation in silica rapidly recombine. Recent ultrafast measurements in crystalline and amorphous SiO_2 estimate the mean lifetime of photogenerated electrons to be on the order of 150 fs.[5] The remaining charge carriers move in the conduction and valence bands, eventually forming excitons or localizing in trap levels.[6−8] These traps are commonly interpreted to be chemical impurities and intrinsic or extrinsic structural defects.[9,10] Silica particles of nanometer dimensions that are suspended in water have additional trapping sites provided by hydroxyl groups that densely populate the surface.[11]

Transfer of radiolytically generated charge carriers across the solid−liquid interface is of great technological significance to the vitrification of radioactive waste.[12] Escape of charges from irradiated particles has important consequences for stored high-level liquid waste, which invariably is heavily loaded with solid particles.[13] Various molecules adsorbed onto metal oxide particles or porous bulk materials have been shown to form radical anions or radical cations or to decompose under the action of ionizing radiation owing to charge migration to the interface.[14] Although the underlying mechanisms are not entirely clear, the adsorbates are believed to interact with surface-trapped charge carriers. As a result, possible applications of ionizing radiation to the degradation of adsorbed environmental pollutants are currently being explored.[15,16] In the present study, however, we ask more fundamental questions: What fraction of the charge carriers, in particular the electrons, which were initially generated in the solid particles is able to escape into the aqueous bulk phase? How does it depend on the dimensions of the particles? Which electrons escape, hot carriers, thermal electrons in the conduction band, or trapped ones?

Absorption of ionizing radiation by water produces hydrated electrons, e^-_{aq}, whose yield decreases during the first few nanoseconds following the absorption of radiation to an ultimate value of 2.8 radicals per 100 eV of absorbed energy.[17] Because it has been very well-characterized, e_{aq}^- provides a convenient tool for examining the fate of radiation energy initially deposited in the aqueous phase or, as is shown in this study, in the solid phase of heterogeneous systems. The yield of electrons escaping irradiated metal oxide particles in aqueous solutions can be studied by monitoring the production of hydrated electrons. Aqueous colloidal dispersions of silica particles remain transparent at least up to 50 wt % SiO_2 and ∼25 nm particle diameter, thereby allowing optical detection of the processes that occur in suspensions upon pulse radiolysis over a wide range of size and composition. We report here the first observation of efficient production of hydrated electrons in aqueous silica suspensions upon absorption of ionizing radiation by the silica particles. Possible mechanisms for the interfacial charge transfer are suggested, and it is hypothesized that hot electrons may exit the SiO_2 particles, effectively channeling the energy deposited in silica to water.

Experimental Section

Chemicals. Three types of Ludox colloidal silica (Aldrich) were used as received: SM-30 (7 nm average particle diameter, stock solutions of 30 wt % SiO_2), HS-40 (12 nm average particle diameter, stock solutions of 40 wt % SiO_2), and TM-50 (22 nm average particle diameter, stock solutions of 50 wt % SiO_2). The largely monodisperse suspensions are basic (pH 9.0−10.2),

* To whom correspondence should be sent.

[†] Present address: University of Notre Dame, The Radiation Laboratory, Notre Dame, IN 46556.

[‡] Present address: Chemistry Department, Brookhaven National Laboratory, Upton, NY 11973.

S1089-5647(98)02129-4 CCC: $15.00
Published on Web 08/20/1998

with negatively charged particles and Na^+ counterions. Suspensions of varying SiO_2 concentrations were prepared by diluting the commercial colloids with water from a Barnstead NANOpure system. Solutions were degassed in 2 cm optical-path Suprasil cells with high-purity nitrogen and sealed just prior to use.

Radiolysis Experiments. Pulse radiolysis of the SiO_2 suspensions was carried out using the Argonne 20 MeV electron linear accelerator (linac). Transient absorption measurements were made using a pulsed xenon lamp as the probe analyzing light with a 60 ps rise-time biplaner phototube detector and a 1 GHz digitizer. Electron pulses of 30 ps in width were utilized in the present study, and the time resolution of the combined system is estimated at 0.3 ns. Each determination of hydrated electron yield is an average of 10 measurements.

Data Analysis Procedures. Details of the convolution procedures used in the determination of initial yields have been previously described.[26] Briefly, solvated-electron yields were determined by convoluting an independently measured system response function with the solution to the appropriate reaction scheme for the first 50 ns of the e^-_{aq} absorption decay at 600 nm. The decay of e^-_{aq} in neat water was fit first using a three-exponential decay law, as is commonly done to model concurrent spur dynamics and homogeneous recombination reactions that occur on comparable time scales. The decay in samples containing silica suspensions were then similarly fit but keeping the rate constants of the fastest two-exponentials (spur part) fixed using the neat water values and varying the other parameters. Using the fit absorption at time zero, along with the cell optical path and known $\epsilon_{600} = 12\,500\ M^{-1}\ cm^{-1}$, we determined the concentration of e^-_{aq} formed immediately following the linac pulse. Results were quantitatively similar when the e^-_{aq} concentration was estimated 10 ns following the linac pulse, long enough for most spur processes to be complete.

Results and Discussion

Expectations. High-energy electrons lose their kinetic energy via interactions either with the electrons or with the nuclei of the medium. For the 20 MeV electrons used in the present experiments, electronic interactions dominate the energy loss mechanism. The cross section for absorption of ionizing radiation can be estimated by the Bethe formula in which the energy loss is directly proportional to the electron density of the irradiated material.[18] As the high-energy electrons produced by the linac pass through the aqueous colloidal suspension of SiO_2 particles, energy is lost via electronic interactions in both the liquid and solid phases in a ratio determined by their relative electron densities and concentration. Thus, as the percentage of solid material increases, so too does the fraction of energy deposited in the solid phase. As alluded to earlier, the interaction of ionizing radiation with either water or silica results in the generation of secondary electrons. The fate of these electrons is dependent on the medium of their creation. If the energy originally deposited in the silica remains in the particles, the total number of hydrated electrons observed in a given volume of sample must decrease upon increasing the weight percent of SiO_2 proportionately with the decrease in the volume fraction of water. If no electrons are transferred from the silica to the water, the concentration of e^-_{aq} will decrease as the lower solid curve in Figure 1, which represents the volume fraction of water in the samples as a function of SiO_2 concentration. This volume fraction, V_{H_2O}, was calculated from the weight percent of SiO_2, w%, and the density of silica in the particles,

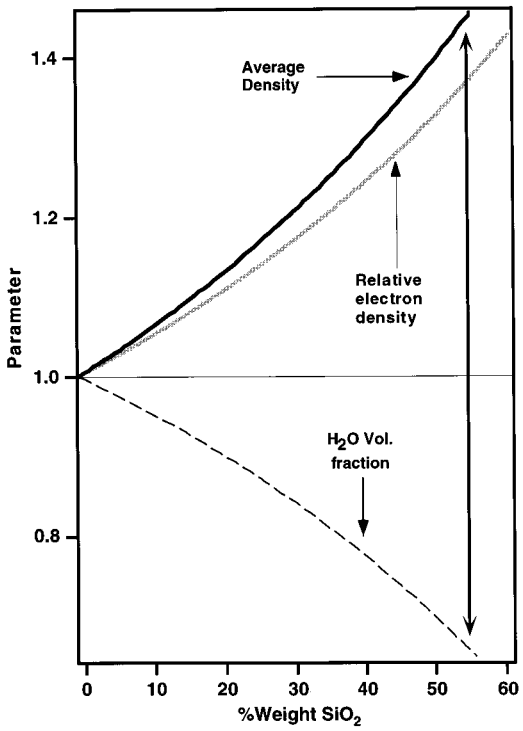

Figure 1. Expectations of e^-_{aq} production from heavily loaded SiO_2/water suspensions. The relative electron density curve represents the increase in absorption of radiation by the sample upon increasing the concentration. Upper solid curve: density approximation. Lower dashed curve: volume fraction of water upon increasing SiO_2 concentration; this curve represents the decrease in absorption of radiation by water. The double arrowed line: fraction of energy absorbed by silica.

$\rho = 2.3\ g\ cm^{-3}$ (and unity for the density of water), using eq 1.

$$V_{H_2O} = \frac{(100 - w\%)\rho}{w\% + (100 - w\%)\rho} \quad (1)$$

There is little doubt that when the particles are large enough, perhaps of macroscopic dimensions, the lower limit curve will be followed. This concept is the principle behind vitrification of nuclear waste.

The relative electron density curve in Figure 1 represents the increase in absorption of radiation by the sample upon increasing the concentration. If absorption of the ionizing radiation energy by the silica nanoparticles is as efficient in generating hydrated electrons as absorption of energy by water, $[e^-_{aq}]$ will follow this curve. The upper solid curve in Figure 1 represents the dependence of the average sample density, ρ_{sm}, on the silica concentration, calculated using eq 2.

$$\rho_{sm} = \frac{100\rho}{w\% + (100 - w\%)\rho} \quad (2)$$

For simplicity it is common to assume that the absorption of energy is proportional to the density of the sample, rather than electron density. At 50% weight of SiO_2 the average density of the suspension is 5% larger than the increase in relative electron density ($1.394\ g/cm^3$ vs 1.324, respectively). The double-arrowed line in Figure 1 shows the fraction of energy that is absorbed in silica. It can be shown that within the "density approximation," this fraction is equal to the weight fraction of silica.

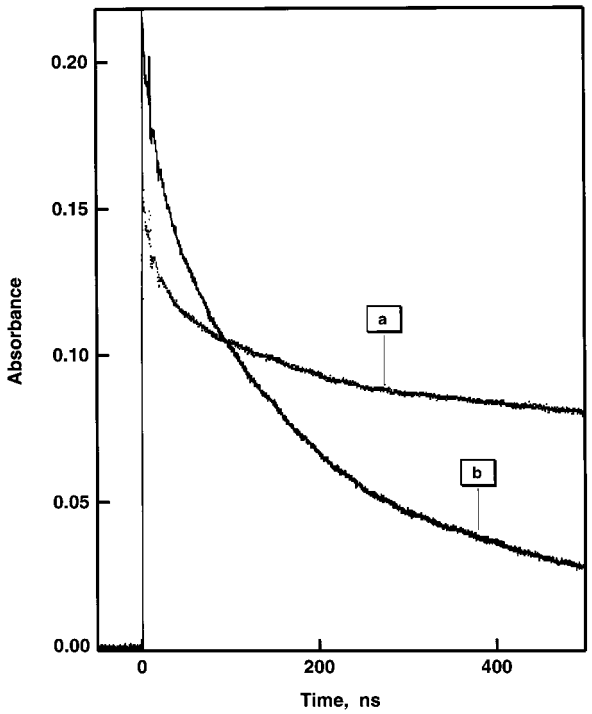

Figure 2. Decay of the hydrated electron absorption (a) in N_2-saturated pure water; (b) in N_2-saturated 40% weight SiO_2 suspension in H_2O.

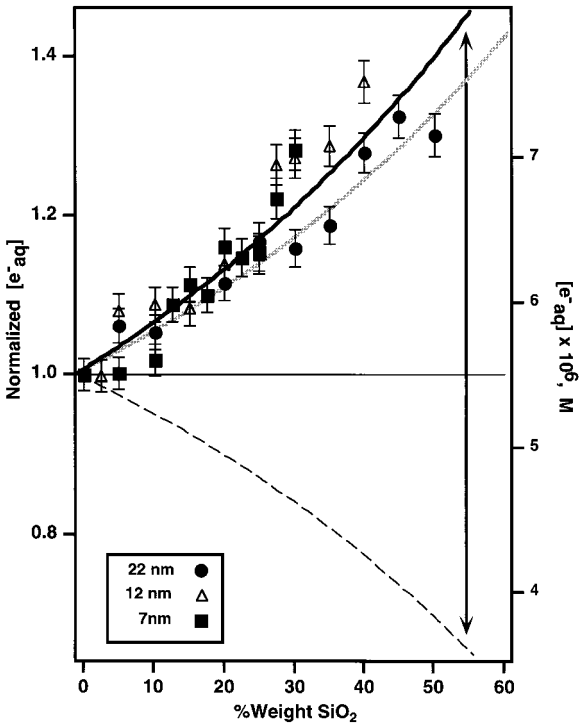

Figure 3. Solvated electrons production from heavily loaded SiO_2/Water suspensions: observations. Curves are from Figure 1. Data points and error estimates for each measurement are shown for 7, 12, and 22 nm particle diameter. Right-hand axis shows the total concentration of e^-_{aq} generated in the cell. The left-hand side axis shows the concentration normalized to the result in pure water. All other curves are as in Figure 1.

Observations and Discussion. Direct time-resolved measurements of the absorption of the hydrated electron in pulse radiolysis experiments over a series of aqueous colloidal silica dispersions were carried out at room temperature. The dynamics of e^-_{aq} formation and decay were followed at 600 nm. Representative absorption transients in water and in a relatively concentrated colloidal solution are shown in Figure 2. The broad absorption spectrum measured in the aqueous silica suspensions is identical within experimental error to the well-known spectrum of the solvated electron in water.[19] No other absorption was observed in the current experiments. The solvated electrons are unlikely to adsorb at the surface of the particles because of their negative surface potential. Taken together with the observation of an identical spectrum as in water, it is reasonable to conclude that the oscillator strength and extinction coefficient of e^-_{aq} are the same as in neat water. Light scattering at 600 nm is minimal. Therefore, problems associated with multiple scattering and possible artifacts that may arise from strong scattering are of little concern in these measurements. Attempts to detect any absorption in the visible range, in the absence of water or in the presence of efficient e^-_{aq} scavengers (acetone, N_2O), revealed none. No absorption in the visible range, owing to trapped species in silica, has been reported in the literature either. Absorption by surface trapped electrons has been reported[11] but was attributed to traps of very negative potentials and therefore would be expected to lead to the solvated state of e^-_{aq}.

The formation of e^-_{aq} throughout this study was prompt, within the time resolution of our equipment, following the electron pulse. Their disappearance extended to the microsecond time regime but is not investigated here in detail. As can be seen in Figure 2, the decay of e^-_{aq} absorption is faster in the suspension than in neat water and is monoexponential. Hydrated electrons are not expected to react with silica because the electrochemical potential of the conduction band in silica is more negative than the redox potential of e^-_{aq} (see Figure 4). Indeed it was established that solvated electrons in water do not react

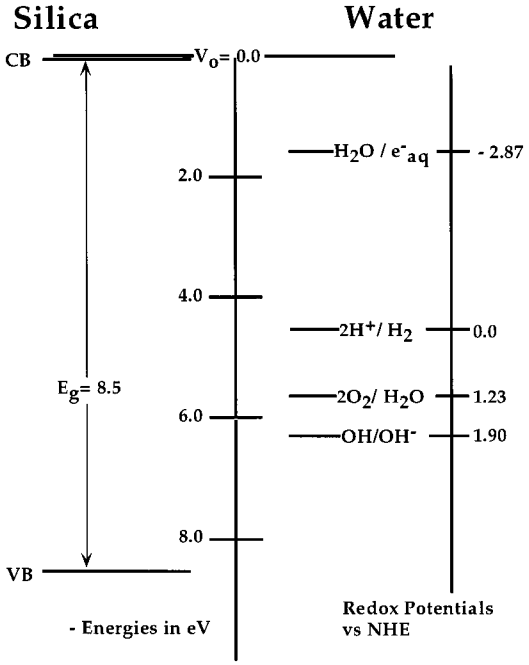

Figure 4. Energy levels and redox potential of some species of interest in this study. Left side are energies on the absolute scale (vacuum level = 0 eV) and right side are redox potentials vs NHE.

with SiO_2 particles.[20] Thus it seems likely that in the presence of high SiO_2 concentrations, the observed faster decay is dominated by reaction with impurities of relatively low concentrations in the heavily loaded suspensions. Most importantly, however, is the observation that the initial concentration of e^-_{aq} is greater in the solution containing the SiO_2 particles. This

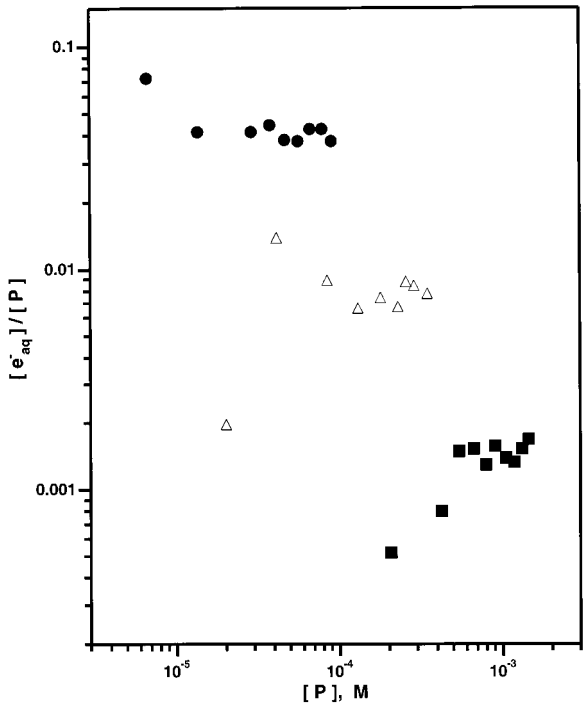

Figure 5. Number of electrons generated in the experiments of Figure 3 per SiO_2 particle. Only those electrons that were initiated by the absorption of energy by the particles are included in the calculation. Symbols of data points are the same as in Figure 3.

result is general throughout the wide range of SiO_2 concentrations and particle sizes examined in this study and will be discussed in detail below.

Initial e^-_{aq} concentrations for three different silica particle sizes, 7, 15, and 22 nm, are superimposed in Figure 3 on the limiting curves from Figure 1. All data points strongly correlate with the sample density curve. One concludes that ionization events initially induced in the particles appear in the water as e^-_{aq} just as efficiently as those that were originally induced in the water. No significant size effect could be discerned. Vestiges of such a dependence are perhaps observable for the largest, 22 nm in diameter, particles. Clearly, the energy that is deposited in the solids is channeled into the aqueous phase; any thermalization, relaxation, or recombination events that occur for electrons in aqueous spurs are as efficient for those that came from ionizations in the silica.

In Figure 5, the experimental observations are cast in terms of the number of hydrated electrons produced per particle. The molar concentration of SiO_2 particles, $[SiO_2]_p$, was calculated from their diameter, d, and the SiO_2 weight percent, using eq 3, where N_0 is Avogadro's number.

$$[SiO_2]_p = \frac{6 \times 10^3 \text{w\%}}{\pi N_0 d^3 \{\text{w\%} + (100 - \text{w\%})\rho\}} \qquad (3)$$

The data shown in Figure 5 have been corrected for the contribution of the aqueous phase to the total concentration of hydrated electrons. Since the fraction of energy deposited in silica equals its weight fraction in the sample (within the density approximation), the observed concentration of e^-_{aq} was multiplied by w%/100 in order to obtain the fraction of electrons originating in the particles. Clearly the yield of e_{aq}^- per particle is well below unity. It should, however, be recognized that the values displayed in Figure 5 represent average concentrations and do not necessarily reflect single ionization events. If electron−hole pairs in silica are generated in localized, occasionally multiionization events, as they are in spurs in water, several electrons may have originated from a single particle regardless of the average concentration. The average spur in water, formed by secondary electrons, corresponds to an energy loss of 20−500 eV in a sphere of ∼2 nm in diameter. The band gap in silica is ∼9 eV, but the lowest energy required for the generation of an electron−hole pair is ∼20 eV.[21] From the approximation of Alig et al.[22] for the average energy required to produce a charge-carrier pair, E_p, one calculates $E_p \approx 2.73E_g + 0.5 = 24$ eV, where E_g is the band gap energy. Therefore, the irradiation of aqueous silica suspensions quite probably leads to the creation of multiple charge carriers in some of the SiO_2 particles and none in most others. With secondary electrons of ∼100 eV, 4−5 electron−hole pairs may be generated in a single particle. A value of 20−25 eV per ionization results in an initial yield of $G = 4-5$ ion pairs per 100 eV, as has been observed for many materials, water included. Whether this yield represents the actual primary initial yield or is merely an observed yield limited by instrumental time resolution is still to be verified.

Once created, several pathways exist for the hot charge carriers to follow. As stated earlier, recombination, exciton formation, and trapping are thought to account for most of the electron−hole pairs within the first few picoseconds of their lifetime. Only a small fraction survives these processes in the bulk, and the yield of free carriers is very small. The adherence of the experimental points in Figure 3 to the "energy absorption" (i.e., density) curve of Figure 1 shows that for small particles, of nanoscale dimensions, escape across the interface into the aqueous phase dominates. From Figure 4 it is clear that solvated electrons cannot "climb" from water into the conduction band in the SiO_2 particles. However, a secondary hot electron initially generated in water could thermodynamically cross into the particle. Such a reverse crossover process will need to occur faster than solvation time of electrons in water, i.e., ∼0.1 ps. Furthermore, the probability for an inverse interfacial transfer is low because of geometrical considerations. The volume fraction of silica is smaller than that of water at a given concentration across the whole set of experiments shown in Figure 3 because of the higher density of silica.

If the secondary electrons created within the silica particle are responsible for the generation of products in the aqueous phase, one expects a particle size effect on the yield of hydrated electrons. There will certainly be a size limit at which the yield will drop; the question is at what dimensions? The results in Figure 3 indicate that the yield of e^-_{aq} is independent of particle diameter over a 7−22 nm range. Taking the radius as the average linear distance traveled by the escaping electrons, one may compare it with results obtained from electron microscopy studies of metal oxide thin films.[23,24] According to these reports, the most probable escape depth is ∼25 nm. Thus, only upon increasing the particle size to about twice the presently utilized largest size might a significant fraction remain (recombine or become trapped) in the particles.

One now wonders which electrons escape into the aqueous phase—hot secondary electrons, thermalized free carriers from the conduction band, or electrons localized in traps of higher energies than the redox potential of e^-_{aq} (Figure 4)? Do these electrons result from energy transfer to the aqueous phase, either as excitonic states or other highly excited states, and subsequently ionize in the water? Preliminary experiments in our laboratory indicate that oxidation equivalents do not migrate across the interface into the water. Rather, they remain in the

silica particles.[25] Therefore, we rule out the possibility that the ionization occurs in water after an energy-transfer process; only the negative charge carriers appear in the water.

Examination of Figure 3 shows that the increase in the "yield" of e^-_{aq} follows the increase in the energy absorption curve. Strictly speaking, taking the term yield to mean the number of electrons generated per unit of energy absorbed by the sample (not merely the aqueous fraction), the yield of solvated electrons actually, and quite surprisingly, remains unchanged. Even though the sample composition has been significantly changed, it behaves entirely as an aqueous sample that absorbs ionizing radiation very efficiently. The double-arrow line in Figures 1 and 3 indicates the fraction of electrons that were initiated by absorption of energy by SiO_2 and escaped into the aqueous phase. Two extreme mechanisms may explain the fact that the expected absorption curve is followed by the experimental results:

(a) All processes that compete with solvation of electrons in pure water are essentially unchanged for electrons that cross into the water from the silica particles. Such a coincidence seems unlikely. Barring unexpected coincidence, this mechanism implies that electrons escaping from the silica are highly energetic and not thermal, free carriers from the conduction band. Their effect, then, is just the same as that of primary electrons for the generation of spurs and secondary electrons in water. Since the lowest ionization in SiO_2 requires at least ~25 eV and since the largest number of secondary electrons in silica appear with a few hundred electronvolts, this proposition is quite plausible.

(b) No recombination and trapping occurs in the silica before escape to the aqueous phase; i.e., all ionizations produce observable solvated electrons. As discussed above, a yield of $G \approx 4.5$ ion pairs per 100 eV may be equivalent to unity yield and is often observed. Since the initial yield of e^-_{aq} is 4.3 radicals per 100 eV,[17] approximately 20 eV are needed to generate a hydrated electron in water, similar to the lowest ionization energy in silica. This mechanism also implies that no recombination occurs prior to observation in neat water as well. Ideally one could distinguish between these two mechanisms by determining the initial yield of other aqueous spur products, such as H atoms or OH radicals. Efforts to obtain such estimates are underway in our laboratory, but in practice this determination is rather difficult.

Practical Implications. The results presented above have many practical implications. Most obviously, storage of nuclear material in an "inert" matrix of small particles (e.g., grout) may lead to adverse effects. If the particles are small, the enhanced absorption of energy in the matrix will lead to more pronounced aqueous radiation chemistry. The observations of the present study may rationalize earlier observations of high H_2 yields from irradiated grout samples.[27] It should, furthermore, be realized that the dependence shown in Figure 3 most probably persists to higher levels of loading. These levels were inaccessible to us in the present study because the samples gel and become opaque; nonetheless, the physical processes are not expected to alter significantly at higher concentrations. At very high concentrations, however, water will become restricted to thin layers around the surface only, and particles may communicate with one another. Then, the yield of e^-_{aq} in the interfacial water may differ from that in bulk water, and furthermore, charge carriers generated in one particle may become trapped in another. At these very high particle concentrations, the radiolysis is expected to change from the behavior observed in Figure 3.

For high-level radionuclides stored in suspensions in large tanks, the presence of the particles will promote generation of water radiolysis products (of particular concern is H_2) in the vicinity of the particles. This may increase the probability of retention of products near the particles, e.g., by gas-bubble attachment to the particle, and may lead to serious safety concerns. On the other hand, ionizing irradiation is often considered as a viable advanced oxidation technique in various cleanup operations, such as water decontamination or soil remediation. Such a radiocatalytic approach, analogous to the proliferating use of photocatalysis, will clearly be most efficient with small particles.

Conclusions

We have demonstrated unequivocally that energy absorbed by solid nanoparticles crosses the solid−liquid interface and generates hydrated electrons as a result of an interfacial charge-transfer process. Subsequently, these electrons will undergo their rich chemical pathways in the aqueous phase. These electrons might be the result of energetic secondary electrons emerging from the silica particles prior to thermalization and having undergone little energy deterioration. Alternatively, if no recombination and trapping occurs in the silica particles (and the aqueous phase) prior to the observation time, the yield of solvated electrons will also follow the observed dependence. Certainly the issue of charge migration in silica particles is relevant to the usefulness of silica-based glassy matrices for high-level waste disposal, but it also bears relevance to many other applications.

The experiments described in this study are hampered by light scattering from the particles. As the size of the particles and their concentration increase, these effects become more severe and the stability of the sol deteriorates. Solvent systems other than water offer an attractive alternative because of their potential for better index matching with SiO_2 ($n_D = 1.457$). Optically matched suspensions would permit a detailed analysis of the size dependence of radiolytic yields. Not only could larger particles be spectroscopically studied, but also higher concentrations of solid material would remain translucent. In preliminary attempts we were able to perform similar experiments at 60% weight SiO_2 in glycerol.

An obvious question that needs to be addressed is the fate of the holes, generated by the radiation together with the electrons. Because the hole mobility in silica is much slower than that of the electrons, it is conceivable that they do not escape the particles prior to deep localization. Preliminary results in our laboratory indicate that this is indeed the case.[25] However, interfacial crossing of hot electrons and generation of secondary spurs requires some increase in the concentration of hole products as well. Other interesting questions that remain to be answered include the effect, if any, of the flat band potentials (i.e., the identity of the material) and surface potential on the interfacial charge-transfer process. We anticipate the latter to be important only at relatively large particle sizes and at electron energies that approach thermalization.

Acknowledgment. Discussions with Drs. J. R. Miller of ANL and T. Orlando of PNNL are greatly appreciated. Support of A.R.C. by the U.S. Department of Energy (DOE), Office of Basic Energy Sciences, Division of Chemical Sciences, and of D.M. and T.S. by the Environmental Management Science Program is gratefully acknowledged. Argonne National Laboratory is operated by the University of Chicago under Contract No. W-31-109-ENG-38 with the DOE.

References and Notes

(1) Spinks, J. W.; Woods, R. J. *An Introduction to Radiation Chemistry*, 3rd ed.; John Wiley & Sons: New York, 1990.

(2) Antonini, M.; Manara, A.; Lensi, P. In *The Physics of SiO_2 and Its Interfaces*; Pantelides, S. T., Ed.; Pergamon Press: New York, 1978; p 316.

(3) Hughes, H. L. In *The Physics and Technology of Amorphous SiO_2*; Devine, R. A. B. Ed.; Plenum Press: New York, 1988; p 455.

(4) Devine, R. A. B. In *The Physics and Chemistry of SiO_2 and the $Si-SiO_2$ Interface*; Helms, C. R.; Deal, B. E. Eds.; Plenum Press: New York, 1988; p 519.

(5) Audebert, P.; Daguzan, P.; Santos, A. D.; Gauthier, J. C.; Geindre, J. P.; Guizard, S.; Hamoniaux, G.; Krastev, K.; Martin, P.; Petite, G.; Antonetti, A. *Phys. Rev. Lett*. **1994**, *73*, 1990.

(6) Vigouroux, J. P.; Duraud, J. P.; Moel, A. L.; Gressus, C. L.; Griscom, D. L. *J. Appl. Phys*. **1985**, *57*, 5139.

(7) Itoh, C.; Tanimura, K.; Itoh, N. *J. Phys. C: Solid State Phys*. **1988**, *21*, 4693.

(8) Itoh, N.; Shimizu-Iwayama, T.; Fujita, T. *J. Non-Cryst. Solids* **1994**, *179*, 194.

(9) DiMaria, D. J. In In ref 2, p 160.

(10) Imai, H.; Hirashima, H. *J. Non-Cryst. Solids*, **1994**, *179*, 202.

(11) Zhang, G.; Mao, Y.; Thomas, J. K. *J. Phys. Chem. B* **1997**, *101*, 7100.

(12) Reference 2.

(13) Lawler, A. *Science* **1997**, *275*, 1730.

(14) Thomas, J. K. *Chem. Rev*. **1993**, *93*, 301 and references cited within.

(15) Hilarides, R. J.; Gray, K. A.; Guzzetta, J.; Cortellucci, N.; Sommer, C. *Environ. Sci. Technol*. **1994**, *28*, 2249.

(16) Mao, Y.; Iu, K. K.; Thomas, J. K. *Langmuir* **1994**, *10*, 709.

(17) Jonah, C. D.; Matheson, M. S.; Miller, J. R.; Hart, E. J. *J. Phys. Chem.* **1976**, *80*, 1267.

(18) Grigoriev, E. I.; Trakhtenberg, L. I. In *Radiation-Chemical Processes in the Solid Phase. Theory and Application* CRC Press: Boca Raton, FL, 1996.

(19) Hart, E. J.; Anbar, M. *The Hydrated Electron*; John Wiley & Sons: New York, 1970.

(20) Lawless, D.; Kapoor, S.; Kennepohl, P.; Meisel, D.; Serpone, N. *J. Phys. Chem*. **1994**, *98*, 9619.

(21) Petr, I. *J. Radioanal. Nucl. Chem.* **1985**, *95*, 195.

(22) Alig, R. C.; Bloom, S.; Struck, C. W. *Phys. Rev. B* **1980**, *22*, 5565.

(23) Kanaya, K.; Ono, S.; Ishigaki, F. *J. Phys. D: Appl. Phys*. **1978**, *11*, 2425.

(24) Seiler, H. *J. Appl. Phys*. **1983**, *54*, R1.

(25) Dimitrijevic, N.; Meisel, D. To be published.

(26) Closs, G. L.; Calcaterra, L. T.; Green, N. J.; Penfield, K. W.; Miller, J. R. *J. Phys. Chem.* **1986**, *90*, 3673.

(27) Jonah, C. D.; Kapoor, S.; Matheson, M. S.; Mulac, W. A.; Meisel, D. *Gas Generation from Hanford Grout Samples*; ANL Report 94/7; Argonne National Laboratory: Argonne, IL, 1994.